Title	Sol-Gel Derived Ti0 $_2$ Film Semiconductor Electrode for Photocleavage of Water : Electrode Reaction Mechanism (Commemoration Issue Dedicated to Professor Tetsuya HANAI On the Occasion of His Retirement)
Author(s)	Yoko, Toshinobu; Yuasa, Akira; Kamiya, Kanichi; Sakka, Sumio
Citation	Bulletin of the Institute for Chemical Research, Kyoto University (1991), 69(4): 311-321
Issue Date	1991-12-30
URL	http://hdl.handle.net/2433/77412
Right	
Type	Departmental Bulletin Paper
Textversion	publisher

Bull. Inst. Chem. Res., Kyoto Univ., Vol. 69, No. 4, 1991.

Sol-Gel Derived TiO_2 Film Semiconductor Electrode for Photocleavage of Water: Electrode Reaction Mechanism

Toshinobu YOKO*, Akira YUASA**, Kanichi KAMIYA** and Sumio SAKKA*

Received august 5, 1991

Photoelectrochemical behavior of TiO_2 (anatase) film electrode prepared by the sol-gel method has been investigated over a wide pH range from 1 to 13.5. It was found that the photocurrent-potential curves in the intermediate pH region comprise the two waves. The first wave dominating above pH=12 was ascribed to the generation of O_2 mainly via H_2O_2 resulting from trapping of the photogenerated holes by Ti^{3+}-OH^-. On the other hand, the second wave dominating below pH=12 was ascribed to the direct photooxidation of water adsorbed at Ti^{3+} sites. On the basis of these results the mechanism that surface states produced by OH^- or H_2O adsorbed at Ti^{3+} sites play an improtant role in photoelectrochemical reaction is proposed.

KEY WORDS: Sol-gel method/ Photoelectrochemistry/ TiO_2 film electrode/ Surface states/ Flat band potential/ Photocurrent

INTRODUCTION

Up to now enormous studies have been carried out on photoelectrochemistry of semiconductor electrodes for wet type solar energy conversion. To obtain new electrode materials with both high efficiency and stability for that purpose[1], the mechanisms of photoelectrochemical reactions at the semiconductor electrode have been also extensively investigated. Especially the surface states (ss) have been known to cause very interesting and significant photoelectrochemical phenomena, such as flat band shift[2-4], Fermi level pinning[5], charge transfer through them[3] and photoluminescence[6], including recombination center as a disadvantage[7].

The authors[8] have recently reported the photoelectrochemical behavior of the TiO_2 film electrodes prepared by the sol-gel method. It was observed that the TiO_2 film electrodes thus prepared show a considerably high photocurrent comparable to a single crystal TiO_2 electrode and a large positive flat band shift under illumination in 0.05mol dm^{-3} H_2SO_4 solution (pH=1). This was explicable by considering that the sol-gel derived TiO_2 films have inherently a large specific surface area and consequently many surface defects, being endowed with a large number of the intrinsic surface states per unit apparent surface area[9].

In the present study, the photoelectrochemical behavior of sol-gel derived TiO_2 film electrodes is investigated over a wide pH range from 1 to 13.5 in order to elucidate the mechanism of photooxidation of water and the role of suface states at the TiO_2

* 横尾 俊信, 作花 濟夫: Laboratory of Ceramic Chemistry, Institute for Chemical Research, Kyoto University, Uji, Kyoto 611, Japan

** 湯浅 章, 神谷 寛一: Department of Chemistry for Materials, Faculaty of Engineering, Mie University, Tsu, Mie-Ken 514, Japan

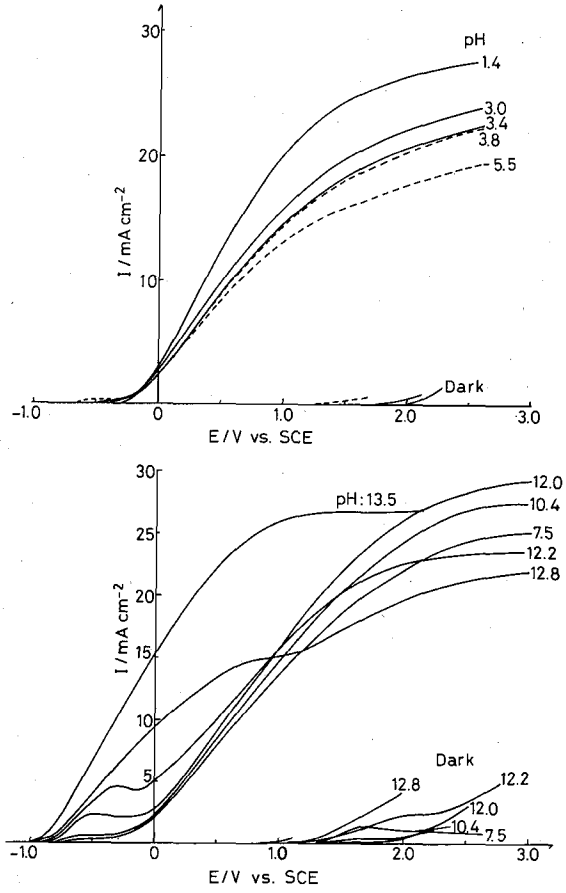

Fig. 1. Photocurrent-bias potential curves at various pH values; scan rate of 20 mVs^{-1}.

semiconductor film electrode.

EXPERIMENTAL

The pH of electrolyte was adjusted by proper comination of H_2SO_4 and NaOH and determined by a digital pH meter (model 3060, Jenway Ltd, England). The TiO_2 (anatase) film used in the present study was 0.9 μm in thickness and subjected to heat-treatment at 600°C for 20 min for high efficiency[9]. Electrochemical mesurements (photocurrent, flat band potential etc.) were conducted in the same manner as described in the previous paper[8].

RESULT

Photocurrent-bias potential (I-E) curves in aqueous solutions at various pH's are shown in Figs. 1a and b. Interesting features are seen from these figures that I-E curves below pH=3.4 show one wave as usual, while above pH=3.8 another new wave (we

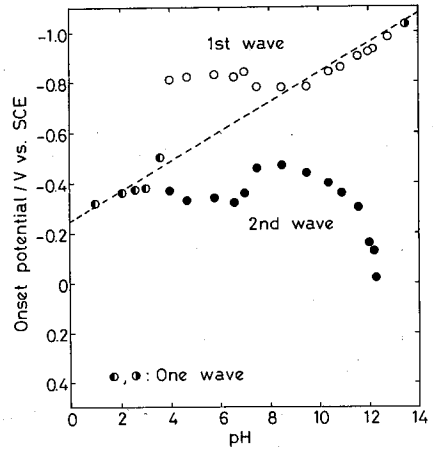

Fig. 2. pH dependences of the onset potential for each wave.

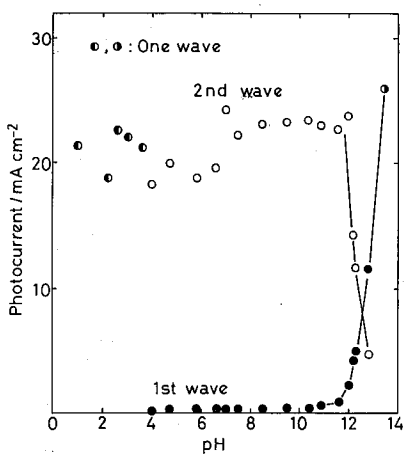

Fig. 3. pH dependences of the photocurrent for each wave in the plateau photocurrent region.

call hereafter the first wave) appears evidently on the negative potential side as shown by broken lines in Fig. 1a for clarity. With increasing pH (Fig. 1b) the first wave grows up at the sacrifice of the wave on the positive potential side (we call hereafter the second wave), which disappears eventually at pH=13.5.

The variations of the onset potentials for respective waves with pH are shown in Fig. 2, where the broken line indicates the pH dependence of evolution potential of hydrogen for comparison. Below pH=3.4 (the second wave) and above pH=9.5 (the first wave), the pH dependences of onset potentials seem to follow the Nernstian law. On the other hand, in the intermediate pH region the onset potentials for both waves seem independent of pH value and above pH=9.5 that for the second wave is shifted unexpectedly toward more positive potentials.

Fig. 3 depicts the pH dependences of photocurrent for respective waves in the plateau region. The second wave is obviously responsible for the total photocurrent up to pH=12, while above pH=12 it becomes drastically smaller, simultaneously accompanied by a sharp enhancement of the first wave photocurrent.

Fig. 4 shows the pH dependences of the flat band potentials V_{fb} in the dark and under illumination. The V_{fb}'s in the dark were measured for some time after the measurements under illumination. It is noteworthy that the pH dependence of V_{fb} in the dark is quite similar to that of the onset potential of the first wave in Fig. 2.

Photocurrent-time responses at several potentials at various pH's are shown in Figs. 5 and 6. At pH's of 1 and 13.5 where only one wave is observed, the evident transient current is not visible (Fig. 5). On the other hand, in the pH region, where two waves are observed, the evident transient current is seen in the vicinity of the onset potential for the second wave (Fig. 6).

DISCUSSION

The existence of the two waves in the I-E characteristics of the single crystal TiO_2

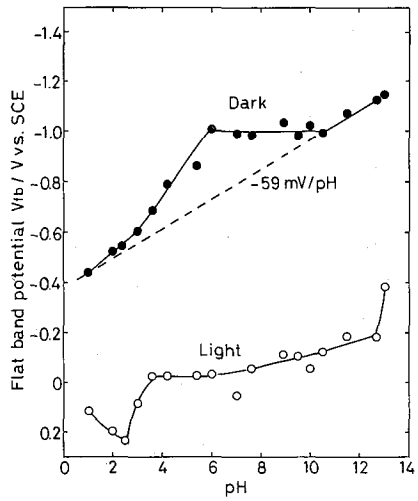

Fig. 4. pH dependences of the flat band potentials in the dark and under ilumination.

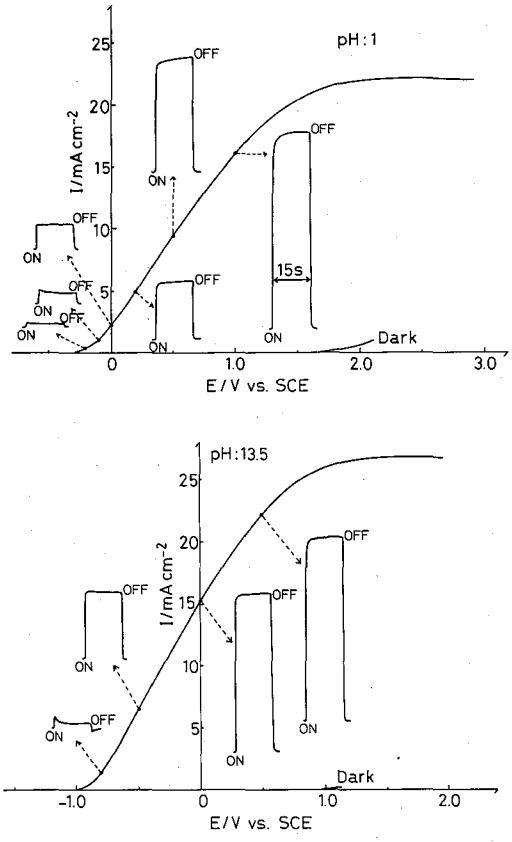

Fig. 5. Photocurrent-bias potential curves and photocurrent-time behavior at several potentials at pH=1 and 13.5.

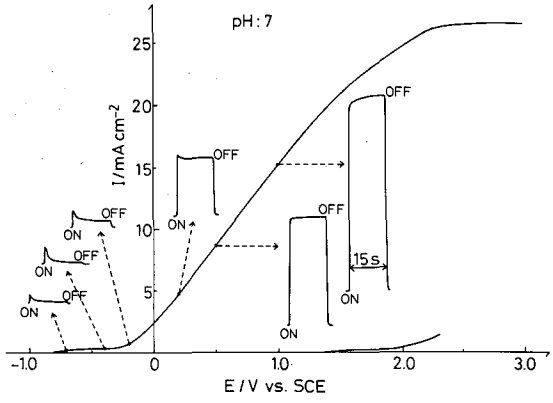

Fig. 6(a)

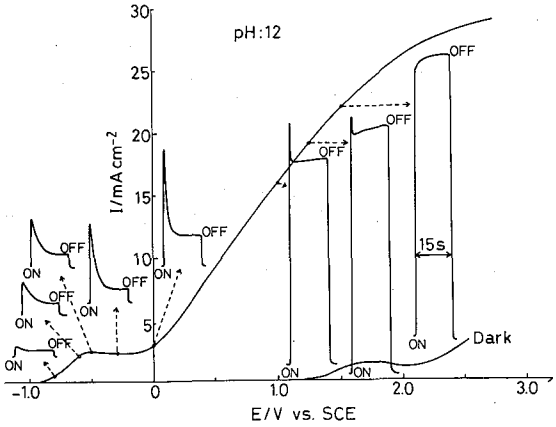

Fig. 6(b)

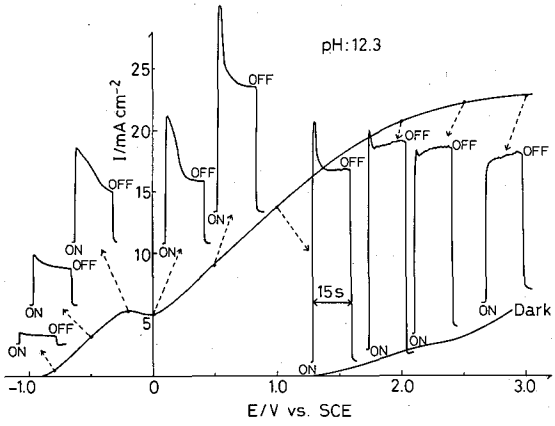

Fig. 6(c)

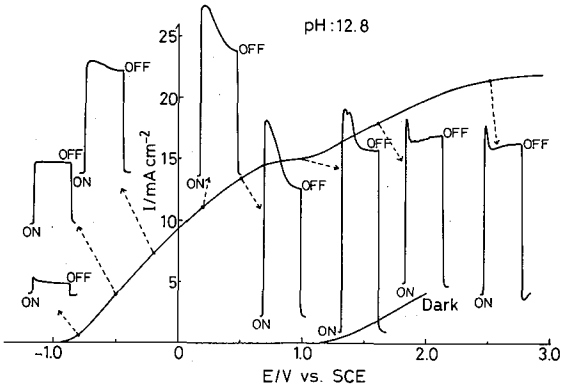

Fig. 6(d)

Fig. 6. Photocurrent-bias potential curves and photocurrent-time behavior at several potentials at pH=7, 12, 12. 3 and 12.8.

(rutile) electrode in the particular pH region was first reported by Despalt[10], although he did not mention any details of this phenomenon in his paper. It is, however, obvious from the present experimental facts that there exist at least two kinds of photocleavage routes for water at the TiO_2 electrode. So the present paper will make clearer the existence and origins of the two waves in the I-E characteristics which were observed for the sol-gel derived TiO_2 (anatase) film electrode in the wide pH region.

The surface of TiO_2 must be in equilibrium with the acidic or basic electroytes as follows[11],

(acidic) $\quad Ti\text{-}OH + H^+ \rightleftharpoons TiOH_2^+$

(basic) $\quad Ti\text{-}OH + OH^- \rightleftharpoons Ti\text{-}O^- + H_2O,$

where the intermediate $TiOH_2^+$ in acidic electrolyte can be taken as for water to be adsorbed at Ti atoms resulting from dissociation equilibrium at the TiO_2— electrolyte interface.

Jaeger and Bard[12] first confirmed the presence of radical intermediates relating to H_2O_2, such as $OH\cdot$ and $HO_2\cdot$ radicals at illuminated TiO_2 powders by spin trapping and ESR techniques. Wilson[13] observed the peaks of dark cathodic current after pre-illumination and assigned them to the reduction of photogenerated H_2O_2. Furthermore, Gutierrez and Salvador[14] ascribed them to the surface states (ss) caused by H_2O_2 forming during preillumination. Following Salvador's experiment the authors[15] have also confirmed experimentally that H_2O_2 forms at the TiO_2 (anatase) film electrode prepared by sol-gel method during illumination in the wide pH range. These things clearly indicate that H_2O_2 is generated by photoelectrochemical reaction at the TiO_2 electrode.

Taking into account these facts, the following two respective reactions are possible in acidic and basic electrolytes as the photooxidation of water by photogenerated holes:

(acidic) $2Ti\text{-}OH_2^+ + 4h^+ \rightarrow 2Ti^+ + 4H^+ + O_2$ ……(1)

$4Ti\text{-}OH_2^+ + 4h^+ \rightarrow 4Ti^+ + 4H^+ + 4OH\cdot$
$4OH\cdot \rightarrow 2H_2O_2 \rightarrow 2H_2O + O_2$ } ……(2)

(basic) $4Ti\text{-}OH + 4h^+ \rightarrow 4Ti^+ + 2H_2O + O_2$ ……(3)

$4Ti\text{-}OH + 4h^+ \rightarrow 4Ti^+ + 4OH\cdot$
$4OH\cdot \rightarrow 2H_2O_2 \rightarrow 2H_2O + O_2$ } ……(4)

The photocurrents must be influenced by the addition of H_2O_2 to the electrolyte, provided eqs.(2) and (4) are prevailing. To confirm the effect of H_2O_2 on each wave, different amounts of H_2O_2 were added to the electrolyte. The results at pH=12.2 are shown in Fig. 7 for an example. The photocurrent values for respective waves in the plateau region are plotted against the H_2O_2 concentration in Fig. 8[15]. As clearly seen from this figure, the second wave dominating in the acidic region shows a less H_2O_2 concentration dependence, while the first wave dominating in the alkaline region strongly depends on the H_2O_2 concentration. That is, the degree of a decrease in the saturation photocurrent is more pronounced for the first wave than for the second wave.

Therefore, it is concluded that the second wave is mainly governed by reaction (1), although reaction (2) cannot be completely ruled out because the formation of H_2O_2 at the TiO_2 (anatase) film electrode after illumination was experimentally confirmed even at pH=1[15]. The above assignment seems in good accordance with the present results that in the higher pH range than 12 the onset potential of the second wave is shifted toward more positive potentials (Fig. 2) and the photocurrent decreases drastically (Fig. 3) due to an increase in concentration overpotential since the number of $TiOH_2^+$ at the surface is considered to decrease with increasing pH. On the other hand, since the first wave is strongly affected by the addition of H_2O_2, reaction (4) is mainly responsible for the first wave.

Lo et al.[16] found based on the UPS study that photoelectrochemical active sites at

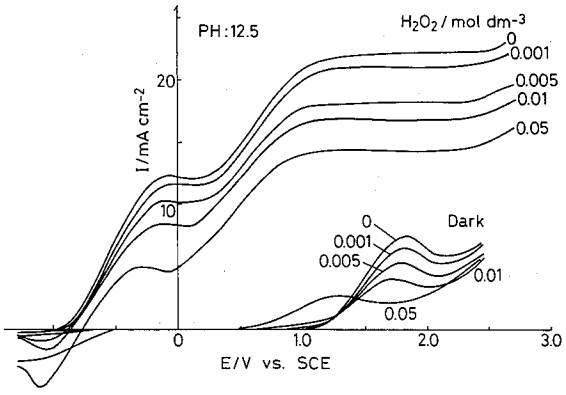

Fig. 7. Variation of photocurrent-bias potential curve at pH12.5 with H_2O_2 concentration.

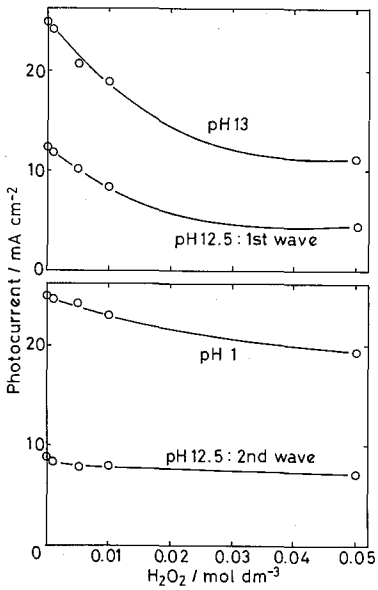

Fig. 8. H_2O_2 concentration dependences of the photocurrent for each wave in the plateau region.

the TiO_2 surface are not Ti^{4+} but Ti^{3+} at which H_2O and/or OH^- are adsorbed. The energy level of Ti^{4+}-OH^- is located at about 0.5eV above the top of valence band[17] but that of Ti^{4+}-H_2O is located far below the top of valence band. On the other hand, those of Ti^{3+}-H_2O and Ti^{3+}-OH^- are located at the band gap of TiO_2 (anatase) electrode[14,16]. Therefore, water and hydroxyl ion adsorbed at Ti^{3+} sites can be oxidized by the photgenerated holes. Schematic energy diagrams and the proposed mechanisms of photoelectrochemical reaction for TiO_2 (anatase) film electrode at several pH's are shown in Fig. 9.

At pH=1, oxygen evolution takes place only via oxidation of water adsorbed at Ti^{3+} on the surface by the photogenerated holes according to reaction (1), giving rise to one wave photcurrent. At pH=7, the number of OH^- is exactly equal to that of H^+ in an electrolyte, leading to an increase in the number of Ti^{3+}-OH^- at the surface. As a result, oxygen evolution via Ti^{3+}-OH^- according to reaction (4) takes place in addition to reaction (1), giving rise to two wave photocurrents. At pH=12, as the number of Ti^{3+}-OH^- increases, the contribution of the first wave to the total photocurrent increases, while the contribution of the second wave decreases. At pH=13.5, as the surface of TiO_2 electrode is considered to be almost competely covered with OH^-, oxygen evolution proceeds exclusively via Ti^{3+}-OH^-, again giving rise to one wave photocurrent only just like at pH=1.

Lo et al.[16] also pointed out that water adsorbs associatively at Ti^{4+} sites, while does dissociatively at Ti^{3+} sites on the surface according to

$$Ti^{3+}+H_2O \rightarrow Ti^{3+}+OH^-+H^+.$$

This may result in giving excess negative charge to the surface independent of equilibrium with an electrolyte especially in the intermediate pH region. As mentioned

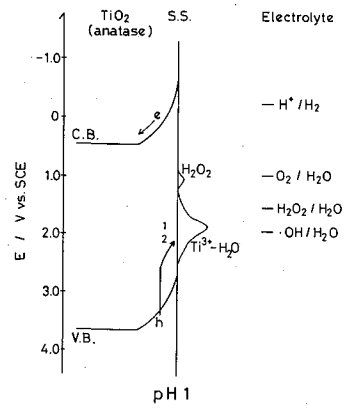

Fig. 9(a)

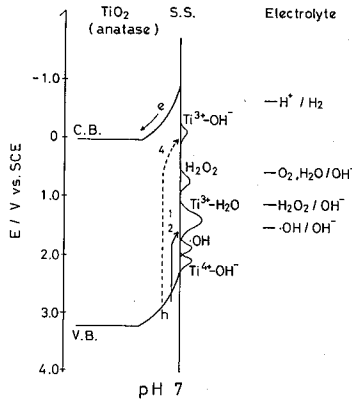

Fig. 9(b)

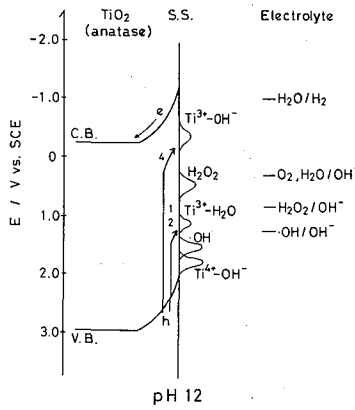

Fig. 9(c)

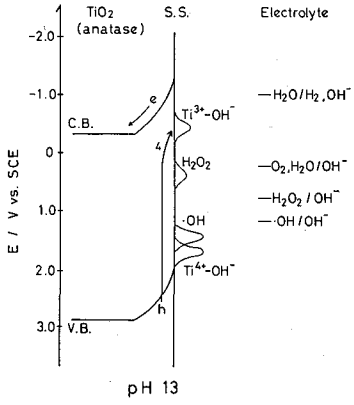

Fig. 9(d)

Fig. 9. Schematic energy diagrams of TiO_2 (anatase)-electrolyte interface at various pH's; (a) pH=1, (b) pH=7, (c) pH=12.2 and (d) pH=13.5.

before, the sol-gel derived TiO_2 film electrodes are characterized by large specific surface area and high donor density (Ti^{3+})[8,9]. These may explain the reason why the onset potenatials of the first wave (Fig. 2) and the V_{fb} in the dark (Fig. 4) are independent of pH in the intermediate pH region. That is, the adsorbed OH^- ions act as potential-determining species in this pH region.

In the pH region where the I-E characteristics show two waves, all the surface states of $Ti^{3+}+OH^-$, $Ti^{3+}+H_2O$, $Ti^{4+}+OH^-$ and adsorbed H_2O_2 at 1.47eV below the bottom of conduction band[18,19] are located between the band gap as shown in Fig. 9b. Thus, in the intermediate pH region there are many surface states by which the photogenerated holes can be trapped.

Fig. 10 depicts relations between the saturation photocurrent and the flat band potential shift ΔV_{fb} which is defined as a difference between the flat band potentials between in the dark and under illumination. Measurements were made at three different light intensities of 300, 400 and 500W. Both the photocurrent and ΔV_{fb} increased with increasing light intensity irrespective of pH. At pH=1, the photocurrent is directly proportional to ΔV_{fb}, which means that all the surface states capable of

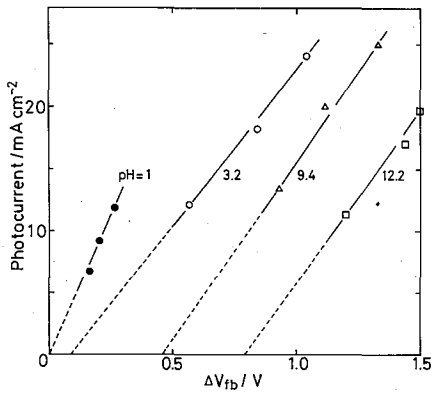

Fig. 10. Relations between ΔV_{fb} and the saturation photocurrent at various pH's. Measurements were made at three different light intensities of 300, 400 and 500W.

trapping the photogenerated holes contribute to the oxidation of water. On the contrary, the higher the pH of the electrolyte, the larger the ΔV_{fb} value at which the photocurrent starts to flow. This indicates that the surface states, which do trap the photogenerated holes but do not take part in the oxidation of water, increase in number with increasing pH.

At shallow bias potential the photogenerated holes are trapped by Ti^{3+}-OH^- due to the largest overpotential with respect to the energy level of hole, causing the photocleavage of water and producing the photocurrent. As the bias potential becomes deeper, in other words, the band bending becomes steeper, the number of photogenerated holes reaching the Ti^{3+}-OH^- surface states increases, because of the suppression of the recombination of photogenerated holes and electrons. When the hole transfer via these surface states attains a steady state, the photogenerated holes become to fill the next deep surface states, in this case Ti^{3+}-H_2O_2,Ti^{3+}-H_2O and Ti^{4+}-OH^-. If the overpotential of photogenerated holes is not enough to oxidize water, these trapped holes may cause a transient photocurrent especially in the vicinity of the onset potential of the second wave in the intermediate pH region as shown in Fig. 6. These results are also quite compatible with the mechanisms proposed in Fig. 9.

ACKNOWLEDGMENT

This work was supported by The Asahi Glass Foundation For Industrial Technology and a Grant-in-Aid for Scientific Reserch from the Ministry of Education, Science and Culture, Japan.

REFERENCES

(1) A. Fujishima, K. Honda and S. Kikuchi, Kogyo-Kagaku Zasshi, *72,* 108 (1969)
(2) Y. Nakato, A. Tsumura and H. Tsubomura, J. Electrochem. Soc., *127,* 1502 (1980)
(3) J.J. Kelly and R. Memming, ibid., *129,* 730 (1982)
(4) P. Allongue, H. Cachet and G. Horowitz, ibid., *130,* 2352 (1983); P. Allongue and H. Cachet, ibid., *132,* 45 (1985)
(5) A.J. Bard, A.B. Biocarsly, Fu-Run F. Fan, E.G. Walton and M.S. Wrighiton, J. Am. Chem. Coc., *102,* 3671 (1980)

(6) Y. Nakato, A. Tsumura and H. Tsubomura, J. Phys. Chem., *87,* 2402 (1983)
(7) R.H. Wilson, J.Appl. Phys., *48,* 4292 (1977)
(8) T. Yoko, K. Kamiya and S. Sakka, Denki-Kagau, *54,* 284 (1986); Yogyo-Kyokai-Shi, *95,* 150 (1987)
(9) T. Yoko, A. Yuasa, K. Kamiya and S. Sakka, J. Electrochem. Soc., *138,* 2308 (1991)
(10) J-L. Despalt, J. Appl. Phys., *47,* 5102 (1976)
(11) P. Boem, Discuss. Faraday Soc., *52,* 264 (1979)
(12) C.D. Jaeger and A.J. Bard, J. Phys. Chem., *84,* 3146 (1979)
(13) R.H. Wilson, J.Electrochem. Soc., *127,* 228 (1980)
(14) C. Gutierrez and P. Salvador, J. Electroanal. Chem., *138,* 457 (1982)
(15) T. Yoko, K. Kamiya, A. Yuasa and S. Sakka, ibid., *209,* 399 (1986)
(16) W.J. Lo, Y.W. Chuang and G.A. Somorjai, Surf. Sci., *71,* 199 (1978)
(17) P. Salvador, J. Phys. Chem., *89,* 3863 (1985)
(18) Y. Nakato, A. Tsumura and H. Tsubomura, ibid., *87,* 2402 (1983)
(19) P. Salvador and C. Gutierrez, ibid., *88,* 3696 (1984)